Nonhuman Primate Models for Diabetic Ocular Neovascularization Using AAV2-Mediated Overexpression of Vascular Endothelial Growth Factor

Corinna Lebherz,[1] Albert M. Maguire,[2] Alberto Auricchio,[3] Waixing Tang,[2] Tomas S. Aleman,[2] Zhangyong Wei,[2] Rebecca Grant,[1] Artur V. Cideciyan,[2] Samuel G. Jacobson,[2] James M. Wilson,[1] and Jean Bennett[2]

Neovascularization leads to blindness in numerous ocular diseases, including diabetic retinopathy, age-related macular degeneration, retinopathy of prematurity, and sickle cell disease. More effective and stable treatments for ocular neovascularization are needed, yet there are major limitations in the present animal models. To develop primate models of diabetic retinopathy and choroidal neovascularization, rhesus monkeys were injected subretinally or intravitreally with an adeno-associated virus (AAV)-2 vector carrying the cDNA encoding human vascular endothelial growth factor (VEGF). Overexpression of *VEGF* was measured by intraocular fluid sampling over time. Neovascularization was evaluated by ophthalmoscopy through angiography, optical coherence tomography, and ultimately histopathology. Overexpression of *VEGF* through AAV2 results in rapid development of features of diabetic retinopathy or macular edema, depending on the targeted cell type/mode of production of VEGF and diffusion of VEGF. Nonhuman primate models will be useful in testing long-term safety and efficacy of novel therapeutic agents for blinding neovascular diseases. *Diabetes* 54:1141–1149, 2005

Diabetic retinopathy is the most common microvascular complication of diabetes, resulting in blindness for >10,000 people with diabetes per year. Chronic diabetes can also result in macular edema, neovascular glaucoma, and neovascularization of the optic disc. There are other conditions in which such pathology can develop, including retinopathy of prematurity, sickle cell retinopathy, and retinal vein occlusion. Diabetic ocular neovascularization and related conditions are leading causes of blindness around the world.

Current treatment options for retinal neovascularization are limited to interventional (1–3) or surgical (4,5) procedures. These treatments are often suboptimal, as they are only suitable for a subset of patients, may stabilize vision loss for only a limited time, and can, themselves, destroy functioning retina. In addition, recurrence of neovascularization is frequent.

Therefore, a number of experimental antiangiogenic therapies have evolved over the last couple of years (rev. in 6). Their aim is to inhibit vessel growth by blocking angiogenic factors like vascular endothelial growth factor (VEGF) using antibodies (7,8), interference RNA (9), or chimeric or soluble VEGF receptor proteins (10,11). Alternatively, they try to induce antiangiogenic activity using enzyme inhibitors (12), fungus-derived antiangiogenic agents (13), or viral vector-mediated delivery of a range of compounds including pigment epithelium–derived factor (14,15), tissue inhibitor of metalloproteinases-3, endostatin, or angiostatin (16).

Even though some of these experimental therapies have been moved to human clinical trials already, the lack of large animal models for ocular neovascularization prevents thorough testing of these substances beforehand. In addition, the paucity of available rodent animal models makes it difficult to select the most appropriate targets for antineovascular therapy.

The challenges with the available animal models include the following. *1*) The method of generation of retinal neovascularization is unrelated to the pathogenic mechanisms causing the human disease (17). *2*) The pathological findings in the laser photocoagulation model, the retinal vein occlusion model, and the retinopathy of prematurity (ROP) mouse model (9,18,19) are only acute and self-limiting, unlike the modeled human diseases. *3*) Neovascular pathology differs from that observed in humans with retinal neovascular disease. In mice transgenic for rhodopsin-promoter VEGF, neovascularization originates from the vitreal side of the retina and emanates to the outer retina (20)—a progression not typically observed in human retinal neovascular disease. *4*) The models lack anatomical features found in primates and humans. Rodents, which are used most commonly for studies of therapeutic efficacy, for example, do not have a macula,

From the [1]Department of Medical Genetics, University of Pennsylvania, Philadelphia, Pennsylvania; the [2]Department of Ophthalmology, F.M. Kirby Center for Molecular Ophthalmology, Scheie Eye Institute, University of Pennsylvania, Philadelphia, Pennsylvania; and the [3]Telethon Institute of Genetics and Medicine, Naples, Italy.

Address correspondence and reprint requests to Jean Bennett MD, PhD, University of Pennsylvania, 310 Stellar Chance Building, 422 Curie Blvd., Philadelphia, PA 190104-6069. E-mail: jebennet@mail.med.upenn.edu.

Received for publication 24 October 2004 and accepted in revised form 3 December 2004.

AAV, adeno-associated virus; AC, anterior chamber; CNV, choroidal neovascularization; EGFP, enhanced green fluorescent protein; NV, neovascularization; OCT, optical coherence tomography; RPE, retinal pigment epithelium; VEGF, vascular endothelial growth factor.

TABLE 1
Summary of the injection route, vector dose, and ocular findings

No.	Route	Dose	Volume	Peak AC fluid VEGF levels (pg/ml): day posttreatment	Clinical-pathological findings	Enucleation of AAV.VEGF-treated eye (day posttreatment/age)
1	s.r.	2.06×10^{12} gc, 6.34×10^{9} ip	150 μl	128: day 35	Retinal NV, cysts, and increased retinal thickness	72 days/6 years
2	i.v.	2.06×10^{12} gc, 6.34×10^{9} ip	150 μl	4,945: day 104	Iris NV and ectropion uveae	ND/5 years
3	s.r.	5.13×10^{11} gc, 3.65×10^{10} ip	200 μl	5,779: day 7	Retinal NV, CNV (23 days), dilation of preretinal vessels cysts, increased retinal thickness	21/3 years
4	i.v.	5.13×10^{11} gc, 3.65×10^{10} ip	200 μl	12,439: day 7	Iris NV, retinal NV, intravitreal hemorrhage, inflammatory cells, enlarged retinal vessels, blisters, and NV at disk	21/4 years
5	None	None		ND	None	None/3 years

gc, genome copies; ip, infectious particles; i.v. intravitreal; ND, not done; s.r., subretinal.

the region of fine visual discrimination affected primarily by human retinal neovascular diseases.

While multiple proangiogenic and antiangiogenic growth factors are likely involved in development and maintenance of the vasculature in the normal eye, aberrant expression of VEGF has received much attention and is thought to play a significant role in the development of ocular neovascularization, such as diabetic retinopathy. High levels of VEGF are present in anterior chamber, vitreous, and tissue samples from humans with diabetic retinopathy, choroidal neovascularization (CNV), and neovascular glaucoma compared with healthy individuals (21–27). Delivery of VEGF protein was therefore a logical approach with which to generate an animal model of retinal neovascularization.

Previous studies in nonhuman primates using repeated intravitreal injections or depot application of VEGF protein were able to reproduce many of the findings of proliferative diabetic retinopathy regarding the inner retinal vessels (28–30). However, intravitreal delivery of VEGF fails to induce macular edema or neovascularization of the outer retina or choroidal plexus. On the other hand, the latter has been induced in another primate model via subretinal delivery of VEGF-impregnated gelatin microspheres, thereby demonstrating the importance of the site of delivery (31). To bypass the need for repetitive injections, several groups have used viral vectors, including adenovirus and adeno-associated virus (AAV) to deliver *VEGF* to retinas of rodents. Such approaches have been successful in rats (32,33) and mice (34–36); however, until now, studies in large animal primates have not been performed.

AAV has been used extensively for gene transfer in the eye. We selected AAV2/2, an AAV possessing the genome and capsids of AAV serotype 2, to deliver the hVEGF cDNA. This virus is able to transduce both cells of the outer retina (photoreceptors, retinal pigment epithelium [RPE] cells, and Muller cells) and inner retina (ganglion cells) depending on the delivery approach (subretinal versus intravitreal injection) and has been shown to enable stable transgene expression in primates (37).

The aim of this study was to produce a nonhuman primate model for ocular neovascularization. The model developed in this study, produced by somatic gene delivery, recapitulates the pathology frequently found in chronic diabetes. Availability of this model will facilitate testing of safety and efficacy of experimental interventions of neovascular blinding diseases.

RESEARCH DESIGN AND METHODS

Vector generation, production, and purification. The human VEGF cDNA (Genbank no. AF486837) was cloned from the Quick-Screen human cDNA library panel (Clontech, Palo Alto, CA) by PCR amplification using the following primers: forward, GCGGCCGCatgaactttctgctgtcttg ggtgcattgg; and reverse, AAGCTTtcaccgcctcggcttgtcacatctgcaagta.

The PCR product was cloned into the pCR2.1 plasmid using the TOPO cloning kit (Invitrogen, Carlsbad, CA) according to manufacturer instructions. After sequence verification, the hVEGF coding sequence was cut from pCR2.1 using *Not*I and *Hind*III and cloned into a pAAV2-cytomegalovirus (CMV) backbone. AAV vectors were produced by triple transfection followed by heparin purification (38). Genome copies were assessed by real-time PCR and infectious copies by the infectious center assay. Expression of VEGF encoded by AAV.VEGF was verified through analyses of the supernatant after transfection of 293 cells using a commercially available enzyme-linked immunosorbent assay kit (R & D Systems, Minneapolis, MN). As control vector, an AAV containing enhanced green fluorescent protein (EGFP) in reverse orientation, AAV.EGFP-RO, was used.

Subretinal and intravitreal injections of rAAV. Animals used in this study were cared for in accordance with institutional and national regulations. Before treatments, baseline ophthalmic examinations, fundus photography and fluorescein angiographies were performed. Complete blood count, serum chemistry, and body weight were obtained before treatment and weekly posttreatment. Anterior chamber fluids were collected at designated time points before and after vector injection.

All procedures were performed using sterile conditions and complete anesthesia. Two monkeys (female rhesus; Covance, Denver, PA) were injected subretinally and two additional ones intravitreally as described (37). The left eyes of all animals were injected with AAV.VEGF and the right eyes with an equal dose of AAV.EGFP-RO. Injection volumes were the same in eyes of the same animals and ranged from 150 to 200 μl in all of the animals. Vector dosages are described in Table 1.

Imaging studies. Animals were followed for up to 1 year after injection (Table 1) and, during the course of this time, received regular clinical examinations including ocular examinations. Changes in retinal and choroidal vasculature were documented through fluorescein angiograms. Photographs were taken with a Kowa Genesis camera (Keeler Instruments, Broomall, PA).

Changes in retinal microstructure of the experimental and control eyes were evaluated in vivo with optical coherence tomography (OCT3; Humphrey Instruments, San Leandro, CA). The principles of the method (39) and our techniques (40,41) have been previously published. Postacquisition processing of OCT data was performed with custom programs (MATLAB 6.5; MathWorks, Natick, MA). Retinal thickness at some loci in the VEGF-treated retina showing loss of signal contrast due to edema was specified manually. A full retinal thickness map was generated by bilinear interpolation and used a pseudocolor scale.

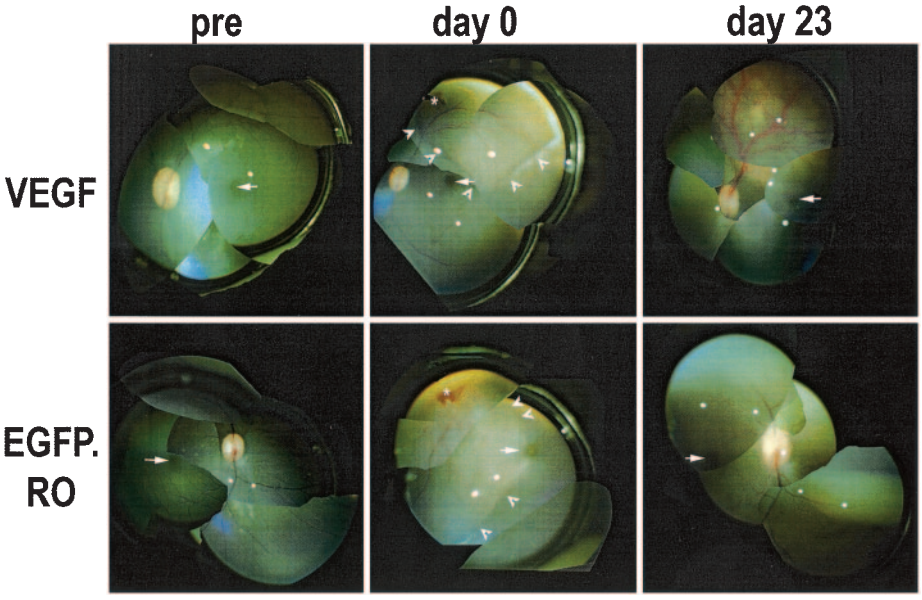

FIG. 1. Fundus photographs before and after subretinal injection of low-dose (6.35×10^9 infectious particles) AAV.VEGF (*A*) or AAV.EGFP-RO (*B*). At day 0, a localized retinal detachment (*arrowheads*) is apparent in the site of injection. This spontaneously reattached within 2 days. Increased vessel thickness and tortuosity are apparent 23 days later in retinal vessels in the area of injection of the AAV-VEGF–treated eye but not in the AAV.EGFP-RO–treated eye. *Arrow*, fovea

Histopathology and immunohistochemistry. Eyes were surgically enucleated at designated time points while animals were under deep anesthesia (isoflurane). (Because the animals were simultaneously enrolled in another unrelated study they were not killed at the time of tissue harvest. In addition, only one eye was harvested per animal.) The eyes were fixed in 4% paraformaldehyde in PBS. The macula and surrounding (uninjected) retina was isolated using a trephine. One-half of the tissue was processed for cryosections, and the other was postfixed in 4% paraformaldehyde and 0.5% glutaraldehyde/PBS before processing for plastic sections. Additional regions in the retinal periphery were processed for cryosections or plastic sections. Cryoprotection was achieved by incubating samples in 30% sucrose/PBS before embedding and freezing in optimal cutting temperature compound (Fisher Scientific, Pittsburgh, PA). Serial sections were cut with a Reichert-Jung model 1800 cryostat (Leica Microsystems, Wetzler, Germany) at 10 μm.

For immunohistochemistry, antibodies against human VEGF (rabbit polyclonal no. A-20 and no. 147; Santa Cruz Biotechnology, Santa Cruz, CA) and 7G6 (mouse monoclonal antibody labeling cone photoreceptors; gift from P. Macleish) were used as primary and the respective fluorescently labeled rabbit and mouse antibodies as secondary (Alexa Fluor 488 and 594; Molecular Probes). Negative controls were performed by omission of the primary antibody. All immunohistochemistry sections were counterstained with 4′,6′-diamidino-2-phenylindole to stain cell nuclei (blue, 1 μg/ml; Molecular Probes).

Sections were evaluated on a Leica DMR microscope, and images were captured with a Hamamatsu charge-coupled device camera (Hamamatsu Photonics, Bridgewater, NJ) coupled to an Apple Macintosh G4 computer (Cupertino, CA) equipped with OpenLab 2.2 software (Improvision, Boston, MA).

RESULTS

Ocular clinical/pathological findings

Subretinal injections. Immediately after subretinal injections of AAV, a "bleb" was observed corresponding to a detachment of the neural retinal from the underlying RPE (Fig. 1, *arrowheads*). The size of the bleb correlated with the injection volume (Table 1). The detachments resolved spontaneously and were no longer apparent within 2 days of the injection. Animals had normal visual behavior, and pupils were reactive to light and symmetrical from eye to eye.

The experimental and control retinas of the animal subretinally treated with the "lower dose" of virus (animal 1, Table 1) were unremarkable in appearance until 21 days after injection. At that point, abnormalities in retinal vasculature were apparent only in the virus-exposed region of the eyes injected with AAV.VEGF but not in the periphery of the same or the control eye (Fig. 1). Fluorescein angiography confirmed the presence of CNV in the experimental but not the control-treated eyes (Fig. 2*A*–*D*). Figure 2*D* shows leakage of fluorescein in the AAV-VEGF–exposed outer retina, while the inner retinal vessels are intact (appearing black, i.e., nonleaky, over the fluorescein-stained outer retina). The leakage occurs only in the region of subretinal injection (compare the circular fluorescein-stained region with the circular region showing retinal vessel changes in Fig. 1, *top panel*, *day 23*).

Similar results were observed in the animal treated subretinally with the higher dose of AAV.VEGF (animal 3, Table 1), except that retinal vasculature abnormalities and CNV were apparent earlier (7 days after treatment) and were more pronounced. Again, there were no abnormalities identified in the anterior segment structures of experimental or control-injected eyes.

Intravitreal injections. In the other cohort, AAV was injected intravitreally directly above the optic nerve head. There were no immediate effects of the injection on the underlying retina/RPE. The retinas were well perfused immediately after the injection and throughout the course of the study.

By 3 weeks after injection of the low vector dose, iris neovascularization was apparent in the eye injected intravitreally with AAV.VEGF (animal 2, Table 1), which was confirmed by fluorescein angiography (Fig. 2*E* and *F*). The pathology slowly progressed, finally leading to a decreased pupillary light reflex and ectropion uveae 8 months after vector injection. There were no signs of retinal neovascularization or CNV in the eye treated with the lower dose of AAV.VEGF over the year that it was studied.

In contrast, local regions of retinal neovascularization were observed in the animal injected intravitreally with the higher titer of AAV.VEGF (animal 4, Table 1) within 7 days of treatment. Fluorescein angiograms documented this retinal neovascularization but had poor resolution due to leakage of fluorescein from the iris neovascularization and a vascularized pupillary membrane, which was present at the same time (Fig. 2*F*). There were no abnor-

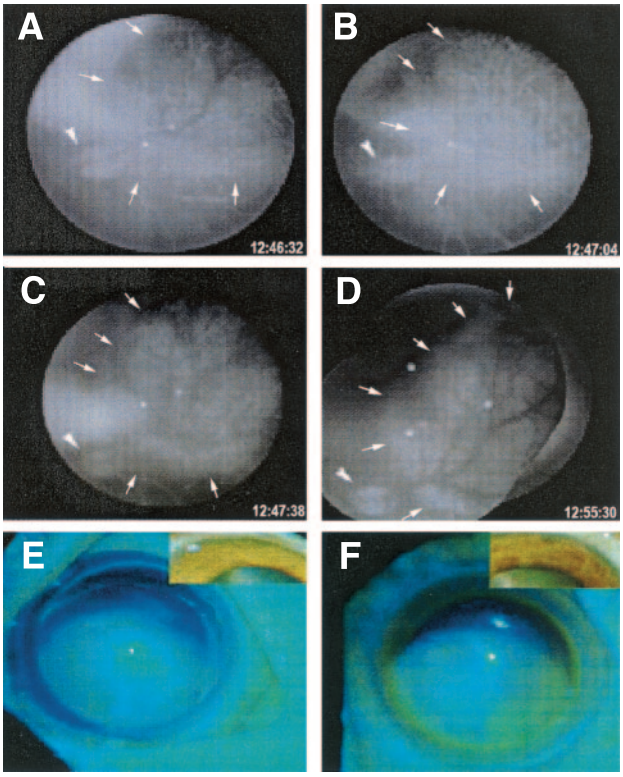

FIG. 2. Fluorescein angiography 4 months after subretinal injection of low-dose AAV.VEGF. CNV was apparent in angiograms (*A–D*) in the region of the eye treated subretinally with AAV.VEGF but not in control or intravitreally injected eyes (data not shown). *Arrowhead*, optic disc. Angiography was performed 4 months after delivery of AAV.VEGF or AAV.EGFP-RO. There was no evidence of vascular leakage before subretinal injection in either eye. Shown in *A–D* are sequential photographs taken during a fluorescein angiogram. Timing of the photograph is indicated on the lower right of each panel. CNV was localized to the retinal site exposed to AAV.VEGF (indicated by *arrows* in *A–D*). The injection site is the same as that depicted in Fig. 1 at day 23 after injection of AAV.VEGF. As time progresses after fluorescein injection (*A–D*), CNV is manifested as presence of dark-appearing inner retinal vessels overlying the diffuse outer retinal fluorescein leakage (outlined by *arrows* in *D*). In eyes injected intravitreally with AAV.VEGF (*F*) but not control virus (*E*) there was extensive iris neovascularization. Insets show color changes (heterochromia) in the experimental (*F*) (but not the control) eye due to iris neovascularization.

malities identified in the anterior segment structures or retinas of the control eyes of these monkeys.

As seen in human diabetic retinopathy in all animals subretinally or intravitreally treated, pathological changes steadily increased over the study period.

Histopathological evaluation

Subretinal injection. Microstructural abnormalities in the retina and their spatial distribution were defined in vivo with OCT, an objective method used increasingly in the clinic to define and safely monitor ocular micropathology in human clinical trials. Scans performed 60 days after a subretinal injection of the low-dose AAV.VEGF preparation showed gross abnormalities in retinal microstructure in the experimental eye compared with the contralateral control eye (Fig. 3). Abnormalities included retinal thickening that was the greatest near the fovea (thickness ~1.3 mm as opposed to ~0.18 mm in the control eye) and extended from there in all meridians (Fig. 3*A*). The extent of abnormalities corresponded approximately to the size of the bleb formed during the subretinal injection. Intraretinal edema and cystic structures and abnormality of the reflections originating from photoreceptor and RPE layers were apparent (Fig. 3*B*). There were no detectable microstructural abnormalities in the control eye that was injected subretinally with the control virus.

Histopathological findings mirrored the results of OCT. Appearance of the regions of the retinas unexposed to AAV.VEGF (i.e., the regions of the retina peripheral to the subretinal injection) were indistinguishable from those of the untreated control monkey. In these regions, there were no alterations in the thicknesses of the various retinal layers or abnormalities in the retinal/choroidal vasculature. There was a sharp boundary between AAV.VEGF-unexposed and -exposed regions, where there were gross abnormalities consisting of large cystic structures and enlarged inner and outer retinal vessels distorting the retinal cell layers and increasing the retinal thickness. In addition, CNV, defined by blood vessels emanating from the choroidal space and traversing Bruch's membrane, and the RPE, was found in numerous

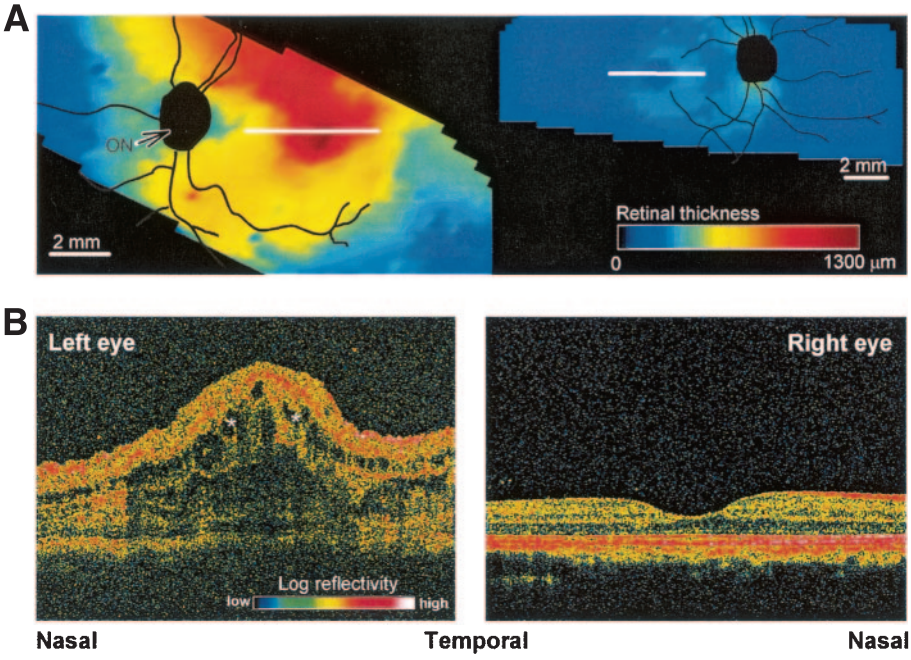

FIG. 3. Optical coherence tomography in the retina injected subretinally with AAV.VEGF. *A*: Topographical map of retinal thickness (pseudocolor map) in the AAV.VEGF-treated left eye shows a large central region of thickening compared with the control virus AAV.EGFP-RO–treated right eye. Horizontal lines in *A* show the location for each panel in *B*. Representative crossectional scans from foveal regions (*B*) show evidence of intraretinal edema and cystic changes in the AAV.VEGF-treated (but not control) retina.

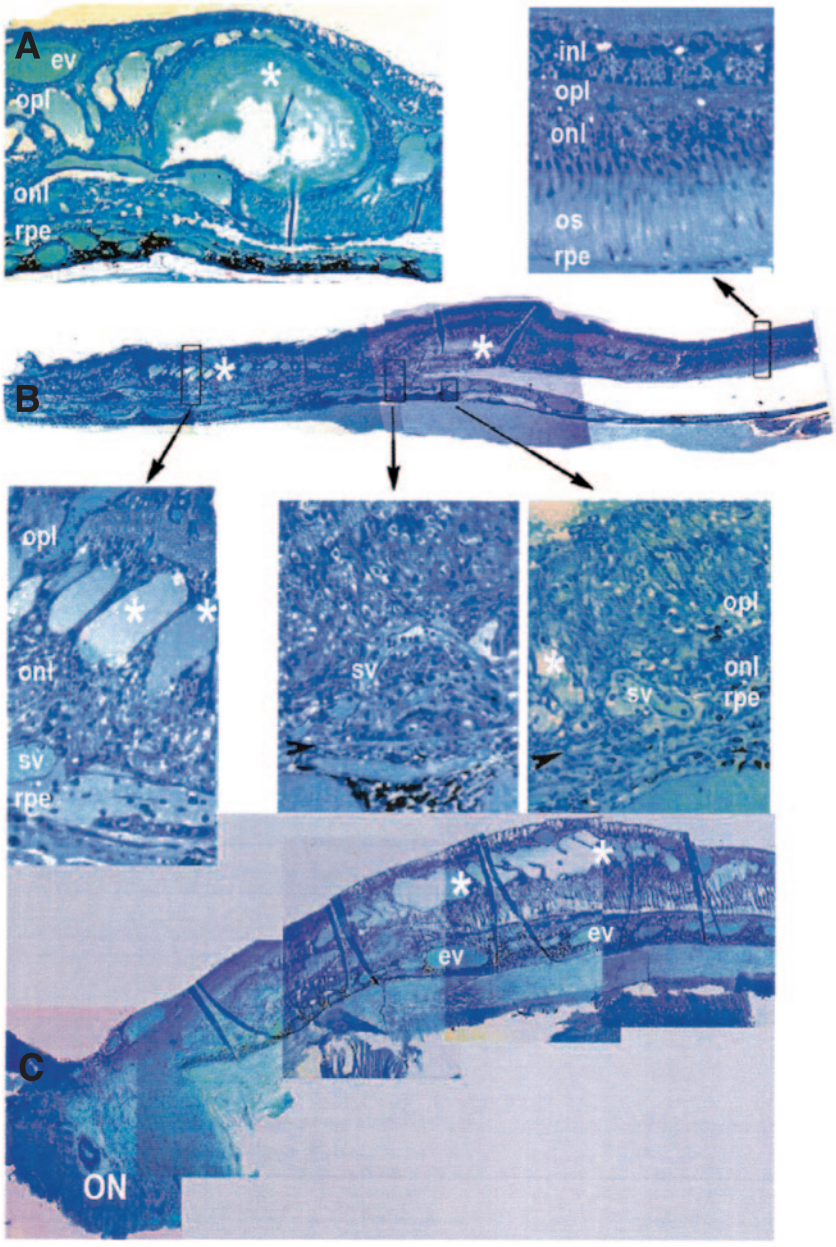

FIG. 4. Histopathological examination after subretinal injection of AAV.VEGF. In the AAV.VEGF-treated region there are dilated (enlarged) blood vessels (ev) in the choroid and neural retina, abnormally located (subretinal) blood vessels (sv), an increase in retina thickness due to edema and cyst formation (*), and alterations in the thicknesses/boundaries of the cell layers of the neural retina. *A* is analogous in location to the region shown in OCT in Fig. 3*B*. *Arrowheads*, Bruch's membrane. inl, inner nuclear layer; ON, optic nerve; onl, outer nuclear layer; opl, outer plexiform layer; os, outer segment; rpe, retinal pigment epithelium.

regions (Fig. 4). These changes are not apparent in the region outside of the subretinal injection site region.

All these changes were accompanied by a disturbance in the architecture of the photoreceptor cells as noted by immunofluorescence. The outer segments were shortened, and the cell bodies were stretched due to the presence of the cystic spaces. There was degeneration of photoreceptor cells as evidenced by decreases in the numbers of these cells, loss of lamination of the retina, and thinning of the outer nuclear, outer plexiform, and outer segment layers.

There was no evidence of changes in thickness or number of blood vessels in anterior segment structures, including the iris and cornea.

Intravitreal injection. Iris neovascularization limited the ability to perform detailed in vivo retinal testing (such as fluorescein angiography, OCT) in the animal intravitreally injected with the high dose of AAV.VEGF. Therefore, the eye was enucleated for histological evaluation. Focal hemorrhages were identified in the iris of this animal in addition to a few blood vessels in the normally avascular cornea. Neovascularization of the optic disc was appreciated. In addition, focal hemorrhagic blister-like regions were observed in the subretinal space of the peripheral retina (Fig. 5). Inflammatory cells were present in high numbers around the retinal blood vessels and in the hemorrhagic regions (data not shown). Despite these changes, there was no retinal degeneration apparent in eyes injected intravitreally with AAV.VEGF.

Detection of transgene expression. After treatment, significantly elevated levels of VEGF were detected in the anterior chamber fluid of every AAV.VEGF-treated eye as compared with titers in the contralateral control eyes using a commercially available enzyme-linked immunosorbent assay kit for human VEGF. Approximately 5- to 20-fold higher VEGF levels were detected in eyes injected intravitreally than in eyes injected subretinally with the same virus/dose of AAV.VEGF. Treatment with the higher dose of vector resulted in a sharp increase in VEGF levels

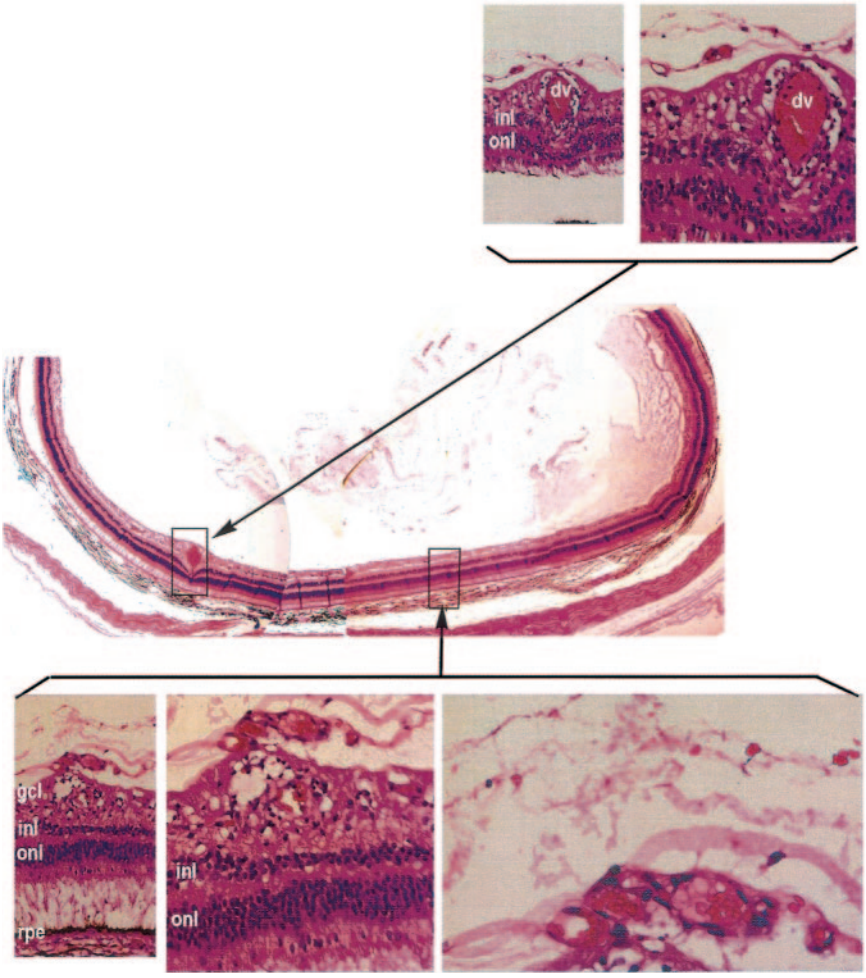

FIG. 5. Pathological effects after intravitreal administration of AAV.VEGF. In the animal treated with the high vector dose, there was retinal neovascularization (appearing as vessels extending vitreally from the retina) and increased diameter of inner retinal vessels (dv). Panels show increasing magnifications of the boxed in regions of the retinal section. Gcl, ganglion cell layer; inl, inner nuclear layer; onl, outer nuclear layer; rpe, retinal pigment epithelium.

followed by a marked drop in levels thereafter, whereas treatment with the lower dose of vector resulted in lower but more stable levels of VEGF, which only slowly declined after a period of several months (Fig. 6).

Immunofluorescence was used to identify cells containing VEGF. VEGF is present endogenously in the ganglion cell layer and in outer segments of photoreceptors in the untreated retina (Fig. 7*A*), and therefore immunofluorescence could only identify qualitative changes in the distribution of VEGF. Twenty-one days after high-dose (Fig. 7*B*) or low-dose subretinal (Fig. 7*C*) AAV.VEGF, VEGF became distributed over the entire photoreceptor cell body and increased relative to baseline in the retinal pigment epithelium. Relative VEGF levels were increased in the ganglion cell layer 21 days after low-dose intravitreal injection of AAV.VEGF (Fig. 7*D*), while high levels of VEGF persisted in photoreceptor outer segments. Relative VEGF levels in photoreceptor outer segments decreased after subretinal injection (Fig. 7*B* and *C*), as many of the expressing cells degenerated and became stretched due to cystoid macular edema.

Systemic effects of ocular treatment with AAV.VEGF. All animals maintained normal activity and maintained their weights throughout the study. Serum clinical chemistry and hematology remained within normal limits. There was no detectable increases in serum VEGF levels in animals treated intraocularly with the lower dose of AAV.VEGF. A slight increase was observed in animals treated with the higher dose of AAV.VEGF, but this was well below levels measured in ocular fluids (data not shown).

DISCUSSION

In this study, ocular neovascularization was induced in nonhuman primates after injection of an AAV2/2 carrying the human VEGF cDNA under control of a constitutive promoter. Two different vector doses and injection routes were chosen to determine the best model imitating the features of diabetic ocular neovascularization as seen in humans.

At a low dose, VEGF gene transfer induced two very different phenotypes, depending on the injection route: iris neovascularization after intravitreous or subretinal neovascularization and cystoid macular edema after subretinal injection. This is surprising because VEGF is a secreted protein and one might expect it to affect multiple locations in the eye through diffusion. However, in other studies where VEGF protein was injected intravitreally, only inner retinal neovascularization (and not subretinal neovascularization) was found (29).

Related to this, we measured close to 20-fold lower levels of VEGF in the anterior chamber fluid after subretinal than after intravitreal injection of the same vector dose. This suggests that VEGF produced after subretinal injection does not readily diffuse across the multilayered retina either because it is too large or because it becomes bound to receptors that are abundant in the outer retina. Interestingly, significantly elevated VEGF protein levels are found in intraocular fluid samples from individuals with inner (but not outer) retinal neovascularization (22–27).

Other potential explanations for the lower VEGF levels

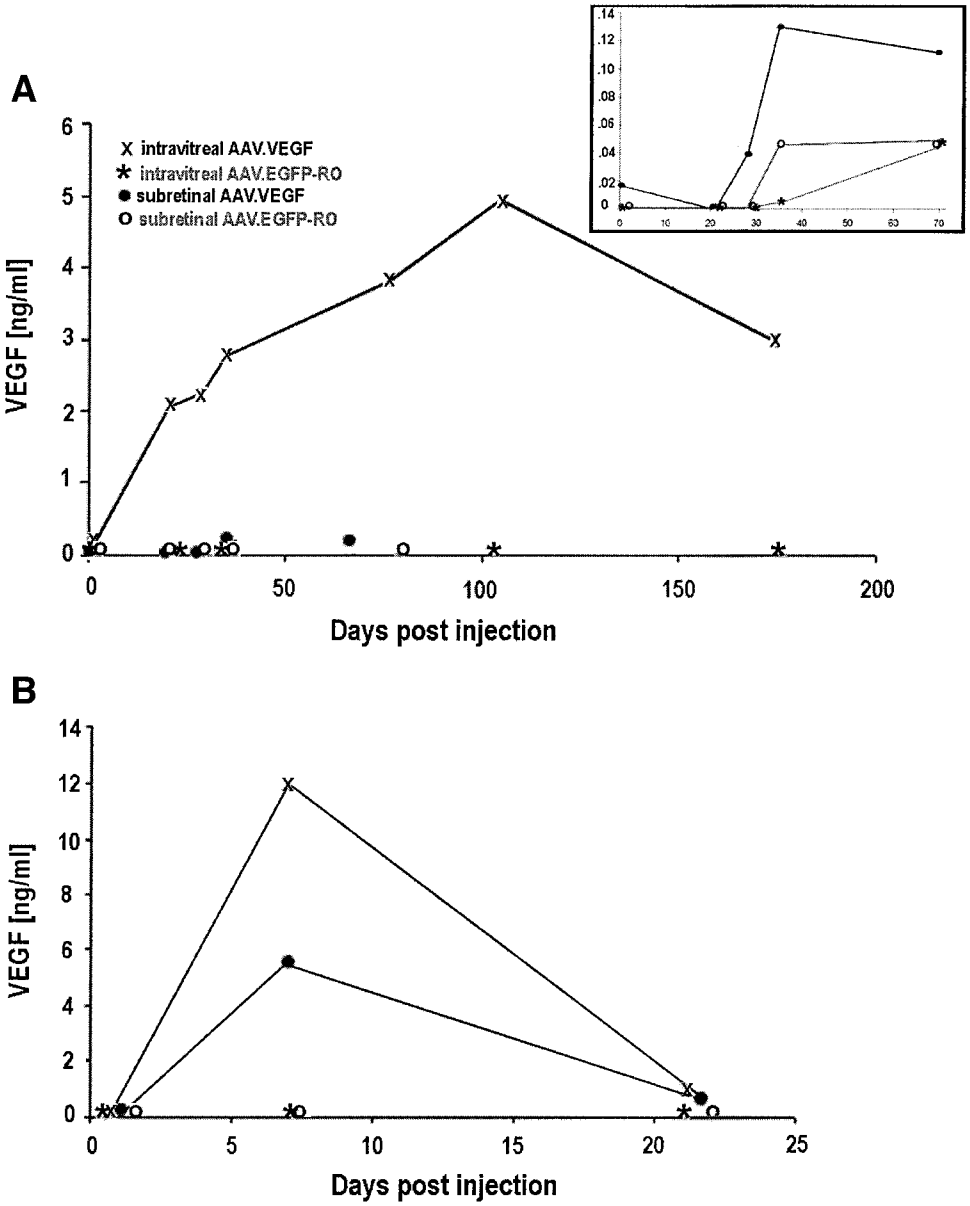

FIG. 6. VEGF levels in the anterior chamber fluid over time after injection. *A*: Dose 1: Intravitreal delivery of 6.35×10^9 infectious particles AAV. VEGF resulted in stable expression of high levels of VEGF starting 21 days after injection. Subretinal delivery of the same dose of virus resulted in a smaller increase in VEGF levels (*inset*). *B*: Dose 2: VEGF levels after delivery of high vector dose (3.65×10^{11} infectious particles) of AAV.VEGF or AAV.EGFP-RO. VEGF levels peaked 7 days after injection and decreased through the 3-week time point in the AAV.VEGF-treated eyes.

we found in anterior chamber fluid samples after subretinal rather than after intravitreal injection would be more efficient transduction or a higher VEGF production level of transduced cells after intravitreal injection due to their own intrinsic activity.

Delivery of high-dose AAV.VEGF induced more rapid and pronounced effects than delivery of low-dose vector. Intravitreal injection led to both iris neovascularization and inner retinal neovascularization within 21 days after injection. Subretinal injection, on the other hand, induced extensive neovascular changes throughout all layers of the retina and the choroid but not in the iris. As seen in the low-vector-dose group, anterior chamber VEGF levels were significantly lower after subretinal than after intravitreal injection. VEGF levels in our study ranged from 0.13 ng/ml to >12.0 ng/ml (shown as pg/ml in Fig. 6) after intravitreal injection of AAV.VEGF and were thus highly comparable with those noted in humans with proliferative retinopathy, reported to range between 0.065, 1.28, and 168,000 ng/ml (22–27).

A surprising finding was the drop in VEGF transgene levels 3 weeks after delivery of a high dose of AAV.VEGF after both intravitreal and subretinal injection. There are several possible explanations for this drop.

First, the very high levels of expression in these eyes may have induced an immune response against the human transgene product. Due to the limited availability of anterior chamber fluid, we were not able to evaluate antibody/cytokine generation. Inflammatory cells were apparent, however, in retinas exposed to the higher doses of AAV.VEGF.

Second, many of the cells targeted by AAV.VEGF may have degenerated due to toxicity of the high concentration of this protein. In support of this, photoreceptor degeneration was apparent in photoreceptors exposed to AAV.VEGF by subretinal injection. Photoreceptors are known to be susceptible to degeneration due to overexpression of proteins, even if those proteins are normally found in these cells (42).

Finally, photoreceptors may have died secondarily to the high levels of serum proteins/erythrocytes that appeared in the retina in response to overexpression of

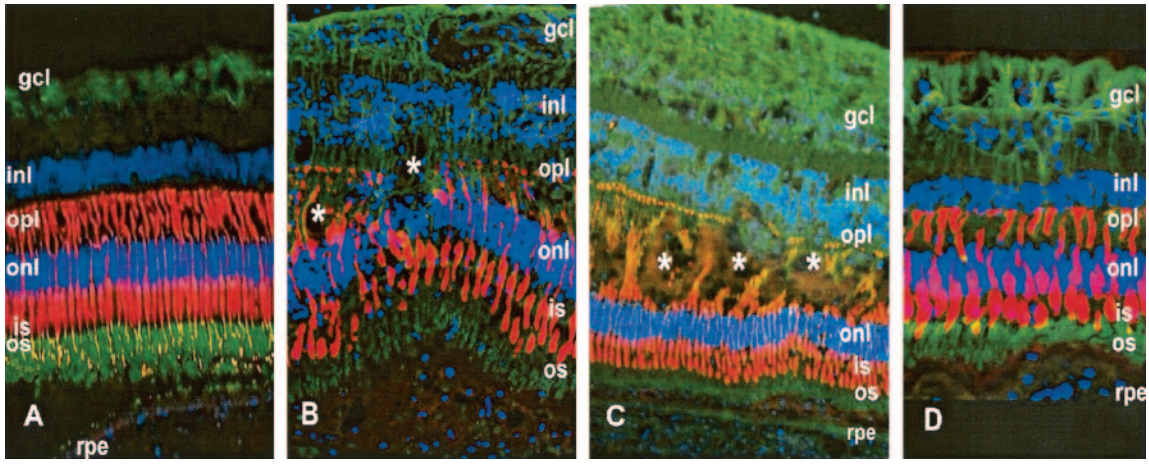

FIG. 7. Immunohistochemical detection of VEGF in experimental and control retinas. VEGF is represented by the green fluorescence, photoreceptors by the red fluorescence, and cell nuclei by the blue fluorescence. In sections from retinas unexposed to virus, VEGF is present primarily in the ganglion cell layer (gcl) and in outer segments (os) of photoreceptors. Twenty-one days after high-dose (*B*) or low-dose subretinal (*C*) AAV.VEGF, VEGF became distributed over the entire photoreceptor cell body and increased relative to baseline in the retinal pigment epithelium (rpe) (compare *C* to *A*). Relative VEGF levels increased in the ganglion cell layer 21 days after low-dose intravitreal injection of AAV.VEGF (*D*). High levels of VEGF were present (as in untreated retina) in photoreceptor outer segments. Relative VEGF levels in photoreceptor outer segments in *B* and *C* were decreased compared with those in *A* and *D* and as many of the expressing cells had degenerated and were stretched due to cystoid macular edema. The ganglion cell layer in *C* appears thick, as this section was taken close to the optic disc and thus possesses a thick nerve fiber layer (made up of ganglion cell axons). inl, inner nuclear layer; is, inner segments; onl, outer nuclear layer; opl, outer plexiform layer; rpe, retinal pigment epithelium. *Cystic changes.

VEGF. Blood cells/serum proteins are known to be toxic to photoreceptors and can induce degeneration within 1 day of exposure (43).

Another unexpected finding in these studies was the high baseline level of VEGF protein in ganglion and photoreceptor cells in untreated monkey retina. Immunohistochemically detectable VEGF levels in these cells were significantly higher than those in RPE cells, retinal vascular endothelial cells, choroidal vessel endothelium, and the inner nuclear layer, in all of which VEGF RNA has been detected previously (44,45). VEGF mRNA is produced by ganglion cells (45); therefore, the presence of VEGF protein in these cells is not surprising. The high levels of VEGF that we observed in photoreceptor outer segments may be due to binding of VEGF to these structures through association with cell-surface proteoglycans. A challenge imposed by the normal VEGF localization pattern in the primate retina is to identify changes in this pattern induced by delivery of AAV.VEGF. Because AAV2 targets the exact same cell types in which VEGF protein is normally present (ganglion cells and photoreceptors) and because our transgene did not contain a biological marker, differences in VEGF levels in our study can only be evaluated by measurements in ocular fluid and alterations in the normal immunohistochemical pattern of VEGF localization. In this study, we observed qualitative increases in VEGF levels in ganglion cells of eyes injected intravitreally and in RPE cells exposed subretinally to AAV.VEGF. Increases of VEGF protein in photoreceptors could not be appreciated due to the severe pathological changes (including cystoid macular degeneration and photoreceptor degeneration) that had taken place in the regions of retina exposed to AAV.VEGF by the time of termination of the study.

In conclusion, we successfully established nonhuman primate models for inner retinal neovascularization, subretinal neovascularization/cystoid macular edema, and iris neovascularization. Iris neovascularization is known to occur in diabetes and can lead to blindness through closure of the irido-corneal angle and concomitant increase in intraocular pressure.

The characteristics and extent of pathology were related directly to the site of AAV.VEGF delivery (and the cells transduced by this virus) and the level of VEGF produced by this treatment. Neovascularization induced via the intravitreal route of delivery of AAV.VEGF simulated diabetic retinopathy, whereas CNV and disturbance of photoreceptor architecture resulted from subretinal injection. Future studies using the intravitreal delivery approach will allow delineation of the pathological mechanisms leading to diabetic retinopathy. In addition, the availability of nonhuman primate models by AAV gene transfer will provide the ability to obtain long-term safety data in an animal model with a macula with respect to efficacy of novel therapeutic compounds designed to treat blinding human retinal neovascular diseases.

ACKNOWLEDGMENTS

This study was supported by the Juvenile Diabetes Research Foundation (to J.M.W. and J.B.), grants R01 EY10820 and EY12156 (to J.B.), grant EY13385 (to S.G.J.), grant EY13203 (to A.V.C.), grant 5-P30-DK-47747-10 from Vector Core Facility (to J.W.), the Foundation Fighting Blindness (to J.B., S.G.J., A.V.C., and T.S.A.), the Lois Pope LIFE (Leaders in Furthering Education) Foundation (to J.B.), the Macula Vision Research Foundation (to S.G.J. and J.B.), The Lew R. Wasserman Award (to J.B.), The William and Mary Greve International Research Scholar Award (to A.V.C.), Research to Prevent Blindness, the Ruth and Milton Steinbach Fund (to J.B.), the Paul and Evanina Mackall Trust, and the F.M. Kirby Foundation.

We thank Joe McLaughlin and Brian Murphy for expert technical assistance and Stuart Fine for review of fluorescein angiograms.

REFERENCES

1. Group MPS: Laser photocoagulation of subfoveal neovascular lesions in age-related macular degeneration: results of randomized clinical trial. *Arch Ophthalmol* 109:1220–1231, 1991
2. Group MPS: Recurrent choroidal neovascularization after argon laser photocoagulation for neovascular maculopathy. *Arch Ophthalmol* 104: 503–512, 1986
3. Group MPS: Persistent and recurrent neovascularization after krypton laser photocoagulation for neovascular lesions of age-related macular degeneration. *Arch Ophthalmol* 108:825–831, 1990
4. Thomas M, Grand M, WIlliams D, Lee C, Pesin S, Lowe M: Surgical management of subfoveal choroidal neovascularization. *Ophthalmology* 99:952–968, 1992
5. Kaplan HJ: Submacular surgery for choroidal neovascularization. *Br J Ophthalmol* 80:101, 1996
6. Bainbridge J, Mistry A, Thrasher A, Ali R: Gene therapy for ocular angiogenesis. *Clinical Sci* 104:561–575, 2003
7. Adamis AP, Shima DT, Tolentino MJ, Gragoudas ES, Ferrara N, Folkman J, D'Amore PA, Miller JW: Inhibition of VEGF prevents ocular neovascularization in a non-human primate. *Arch Ophthalmol* 114:66–71, 1996
8. Group ES: Anti-vascular endothelial growth factor therapy for subfoveal choroidal neovascularization secondary to age-related macular degeneration: phase II study results. *Ophthalmol* 110:979–986, 2003
9. Reich S, Fosnot J, Kuroki A, Tang W, Yang X, Maguire A, Bennett J, Tolentino M: Small interfering RNA targeting VEGF effectively inhibits ocular neovascularization in a mouse model. *Mol Vision* 9:210–216, 2003
10. Aiello LM, Pierce E, Foley E, Takagi H, Chen H, Riddle L, Ferrara N, King G, Smith L: Susppression of retinal neovascularization in vivo by inhibition of vascular endothelial growth factor (VEGF) using soluble VEGF-receptor chimeric proteins. *Proc Natl Acad Sci U S A* 92:10457–10461, 1995
11. Bainbridge JW, Mistry A, De Alwis M, Paleolog E, Baker A, Thrasher AJ, Ali RR: Inhibition of retinal neovascularisation by gene transfer of soluble VEGF receptor sFlt-1. *Gene Ther* 9:320–326, 2002
12. Danis R, Bingaman D, Jirousek M, Yang Y: Inhibition of intraocular neovascularization caused by retinal ischemia in pigs by pkc inhibition with LY333531. *Invest Ophthalmol Vis Sci* 39:171–179, 1998
13. Kusaka M, Sudo K, Fujita T, Marui S, Itoh F, Ingber D, Folkman J: Potent anti-angiogenic action of AGM-1470: comparison to the fumagillin parent. *Biochem Biophys Res Comm* 174:1070–1076, 1991
14. Ishida K, Yoshimura N, Mandai M, Honda Y: Inhibitory effect of TNP-470 on experimental choroidal neovascularization in a rat model. *Invest Ophthalmol Vis Sci* 40:1512–1519, 1999
15. Mori K, Duh E, Gehlbach P, Ando A, Takahashi K, Pearlman J, Mori K, Yang HS, Zack DJ, Ettyreddy D, Brough DE, Wei LL, Campochiaro PA: Pigment epithelium-derived factor inhibits retinal choroidal neovascularization. *J Cell Physiol* 188:253–263, 2001
16. Mori K, Gehlbach P, Yamamoto S, Duh E, Zack DJ, Li Q, Berns KI, Raisler BJ, Hauswirth WW, Campochiaro PA: AAV-mediated gene transfer of pigment epithelium-derived factor inhibits choroidal neovascularization. *Invest Ophthalmol Vis Sci* 43:1994–2000, 2002
17. Meneses P, Hajjar K, Berns K, Duvoisin R: Recombinant angiostatin prevents retinal neovascularization in a murine proliferative retinopathy model. *Gene Ther* 8:646–648, 2001
18. Dobi ET, Puliafito CA, Destro M: A new model of experimental choroidal neovascularization in the rat. *Arch Ophthalmol* 107:264–269, 1989
19. Penn J, Henry M, Tolman B: Exposure to alternating hypoxia and hyperoxia causes severe proliferative retinopathy in the newborn rat. *Ped Res*:724–731, 1994
20. Cunningham S, McColm J, Wade J, Sedowofia K, McIntosh N, Fleck B: A novel model of retinopathy of prematuritiy simulating preterm oxygen variability in the rat. *Invest Ophthalmol Vis Sci* 41:4275–4280, 2000
21. Okamoto N, Tobe T, Hackett S, Ozaki H, Vinores M, LaRochelle W, Zack D, Campochiaro P: Transgenic mice with increased expression of vascular endothelial growth factor in the retina: a new model of intraretinal and subretinal neovascularization. *Am J Pathol* 151:281–291, 1997
22. Aiello L, Avery R, Arrigg P, Keyt B, Jampel H, Shah S, Pasquale L, Thieme H, Iwamoto M, Park J, et al.: Vascular endothelial growth factor in ocular fluid of patients with diabetic retinopathy other retinal disorders. *N Engl J Med* 331:1480–1487, 1994
23. Wells J, Murthy R, Chibber R, Nunn A, Molinatti P, Kohner E, Gregor Z: Levels of vascular endothelial growth factor are elevated in the vitreous of patients with subretinal neovascularization. *Br J Ophthalmol* 80:363–366, 1996
24. Mitamura Y, Tashimo A, Nakamura Y, Tagawa H, Ohtsuka K, Mizue Y, Nishihara J: Vitreous levels of placenta growth factor and vascular endothelial growth factor in patients with proliferative diabetic retinopathy. *Diabetes Care* 25: 2352, 2002
25. Ogata N, Nishikawa M, Nishimura T, Mitsuma Y, Matsumura M: Unbalanced vitreous levels of pigment epithelium-derived factor and vascular endothelial growth factor in diabetic retinopathy. *Am J Ophthalmol* 134: 348–353, 2002
26. Adamis AP, Miller J, Bernal M, D'Amico D, Folkman J, Yeo TK, Yeo KT: Increased vascular endothelial growth factor levels in the vitreous of eyes with proliferative diabetic retinopathy. *Am J Ophthalmol* 118:445–450, 1994
27. Kvanta A, Algvere P, Berglin L, Seregard S: Subfoveal fibrovascular membranes in age-related macular degeneration express vascular endothelial growth factor. *Invest Ophthalmol Vis Sci* 37:1929–1934, 1996
28. Miller JW, Adamis AP, Shima DT, D'Amore PA, Moulton RS, O'Reilly MS, Folkman J, Dvorak HF, Brown LF, Berse B, et al.: Vascular endothelial growth factor/vascular permeability factor is temporally spatially correlated with ocular angiogenesis in a primate model. *Am J Pathology* 145:574–584, 1994
29. Tolentino MJ, McLeod D, Taomoto M, Otsuji T, Adamis A, Lutty G: Pathologic features of vascular endothelial growth factor-induced retinopathy in the nonhuman primate. *Am J Ophthalmol* 133:373–385, 2002
30. Ozaki H, Hayashi H, Vinores SY, Campochiaro P, Oshima K: Intravitreal sustained release of VEGF causes retinal neovascularization in rabbits and breakdown of the blood-retinal barrier in rabbits and primates. *Exp Eye Res* 64:505–517, 1997
31. Cui J, Kimura H, Spee C, Thumann G, Hinton D, Ryan S: Natural history of choroidal neovascularization induced by vascular endothelial growth factor in the primate. *Graefe's Arch Clin Exp Ophthalmol* 238:326–333, 2000
32. Wang F, Rendahl K, Manning WD, Coyne M, Miller S: AAV-mediated expression of vascular endothelial growth factor induces choroidal neovascularization in rat. *Invest Ophthalmol Vis Sci* 44:781–790, 2003
33. Robinson LM, Baffi JS, Yuan P, Sung C-H, Dedrick R, Byrnes G, Cox T, Csaky K: Safety and pharmacokinetics of intravitreal 2-methoxyestradiol implants in normal rabbit and pharmacodynamics in a rat model of choroidal neovascularization. *Exp Eye Res* 74, 2001
34. Rakoczy PE, Brankov M, Fonceca A, Zaknich T, Rae BC, Lai CM: Enhanced recombinant adeno-associated virus-mediated vascular endothelial growth factor expression in the adult mouse retina: a potential model for diabetic retinopathy. *Diabetes* 52:857–817, 2003
35. Baffi JS, Byrnes G, Chan CC, Csaky KG: Choroidal neovascularization in the rat induced by adenovirus mediated expression of vascular endothelial growth factor. *Invest Ophthalmol Vis Sci* 41:3582–3589, 2000
36. Yu M, Shen W, Lai M, Constable I, Rakoczy P: Generation and characterization of a recombinant adenovirus expressing vascular endothelial growth factor for studies of neovascularization in the eye. *Aust N Z J Ophthalmol* 27:250–253, 1999
37. Bennett J, Maguire AM, Cideciyan AV, Schnell M, Glover E, Anand V, Aleman TS, Chirmule N, Gupta AR, Huang Y, Gao GP, Nyberg WC, Tazelaar J, Hughes J, Wilson JM, Jacobson SG: Recombinant adeno-associated virus-Mediated gene transfer to the monkey retina. *Proc Natl Acad Sci U S A* 96:9920–9925, 1999
38. Auricchio A, Hildinger M, O'Connor E, Gao G-P, Wilson J: Isolation of highly infectious and pure AAV2 vectors with a single-step gravity-flow column. *Human Gene Ther* 12:71–76, 2001
39. Huang D, Swanson EA, Lin CP, Schuman JS, Stinson WG, Chang W, Hee MR, Flotte T, Gregory K, Puliafito CA, et al.: Optical coherence tomography. *Science* 254:1178–1181, 1991
40. Huang Y, Cideciyan A, Papastergiou G, Banin E, Semple-Rowland S, Milam A, Jacobson S: Relation of optical coherence tomography to microanatomy in normal and rd chickens. *Invest Ophthalmol Vis Sci* 39:2405–2416, 1998
41. Kijas J, Cideciyan A, Alemand T, Pianta M, Pearce-Kelling S, Miller B, Jacobson S, Aguirre G, Acland G: Naturally occurring rhodopsin mutation in the dog causes retinal dysfunction and degeneration mimicking human dominant retinitis pigmentosa. *Proc Natl Acad Sci U S A* 99:6328–6333, 2002
42. Olsson J, Gordon J, Pawlyk B, Roof D, Hayes A, Molday R, Mukai S, Cowley G, Berson E, Dryja T: Transgenic mice with a rhodopsin mutation (Pro23His): a mouse model of autosomal dominant retinitis pigmentosa. *Neuron* 9:815–830, 1992
43. Glatt H, Machemer R: Experimental subretinal hemorrhage in rabbits. *Am J Ophthalmol* 94:762–773, 2002
44. Lutty GA, McLeod DS, Merges C, Diggs A, Plouet J: Localization of vascular endothelial growth factor in human retina and choroid. *Arch Ophthalmol* 114:971–977, 1996
45. Kim I, Ryan A, Rohan R, Amano S, Agular S, Miller J, Adamis A: Constitutive expression of VEGF, VEGFR-1 and VEGFR-2 in normal eyes. *Invest Ophthalmol Vis Sci* 40:2115–2121, 1999